

PbTiO₃(001) Capped with ZnO(11 $\bar{2}$ 0): An Ab-Initio Study of Effect of Substrate Polarization on Interface Composition and CO₂ Dissociation

Babatunde O. Alawode and Alexie M. Kolpak*
 Massachusetts Institute of Technology, Cambridge, MA 02139
 (Dated: March 1, 2022)

Catalytic conversion of CO₂ into useful chemicals is an attractive alternative to expensive physical carbon sequestration methods. However, this approach is challenging because current chemical conversion methods employ high temperatures or pressures, thereby increasing cost and potentially leading to net carbon positive processes. In this paper, we examine the interface properties of ZnO(11 $\bar{2}$ 0)/PbTiO₃ and its surface interaction with CO₂, CO and O. We show that the stoichiometry of the stable interface is dependent on the substrate polarization and can be controlled by changing the growth conditions. Using a model reaction, we demonstrate that a dynamically tuned catalysis schemes could enable significantly lower-energy approaches for CO₂ conversion.

Catalytic conversion of CO₂ into fuels or other materials that can be used on an industrial scale is an attractive alternative to expensive carbon capture and sequestration (CCS) methods currently under consideration. As CCS is only feasible when large quantities of CO₂ are generated, preferably close to a suitable geological formation [1], this option cannot be used to address the emissions sources with the greatest collective impact: vehicles and small industrial plants. In contrast, since CO₂ can be used a precursor for the synthesis of numerous, industrially relevant carbon based compounds, chemical sequestration approaches could in principle be tailored to smaller scale applications, with implementation costs offset by the production of value-added chemicals. Although conceptually appealing, chemical conversion approaches are challenging due to the exceptional stability of the CO₂ molecule. As a result, CO₂ conversion reactions are performed under energetically costly conditions (i.e., high temperature and/or high pressure) that mitigate the effects of chemical sequestration; in fact, this can lead to some reactions being net carbon positive, generating more CO₂ than they consume [2]. In order to make chemical sequestration feasible, new catalysts that can operate under low temperature and pressure conditions need to be developed.

Various studies have shown that the polariza-

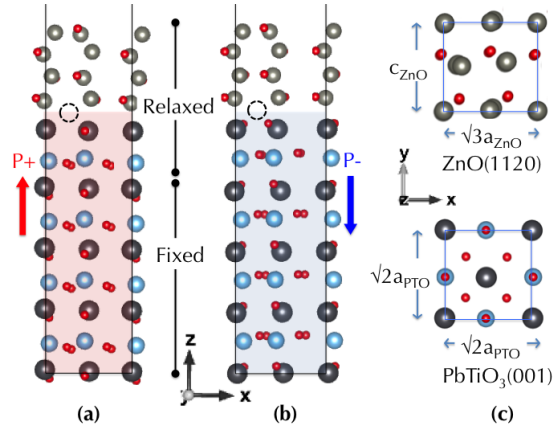


FIG. 1. Computation supercell and relaxed atomic structure for (a) ZnO(11 $\bar{2}$ 0)_n/PbTiO₃[↑] and (b) ZnO(11 $\bar{2}$ 0)_n/PbTiO₃[↓] slabs for $n = 4$. The dashed circle represents the position for oxygen insertion at the interface. Fig. (c) shows the parameters and orientations for matching ZnO(11 $\bar{2}$ 0) to PbTiO₃(001). Grey, red, cyan, and black atoms are Zn, O, Ti, and Pb, respectively.

tion of a substrate can affect its surface properties [3, 4], and this effect has been applied to studies of molecular adsorption [5–8] and the modulation of the carrier density in conductors [9]. Kolpak *et al.* suggested the possibility of using dynamical control of surface structure and reactivity in the coupling of ferroelectric PbTiO₃ with Pt [10]. Performing density func-

tional theory (DFT) computations of molecular and atomic adsorption to the surface of ultrathin Pt(100) films supported on ferroelectric PbTiO_3 , they showed that switching the polarization direction of the substrate dramatically changes the chemisorption strength and site preference of CO, O, C, and N, potentially altering the reaction pathways for dissociation of CO, O_2 , N_2 and NO. However, polarization-induced changes in the surface chemistry effects are mitigated by the small electronic screening length of Pt, so that only atomically thick films exhibit significant effects. Moreover, it is challenging to wet oxide surfaces with catalytically active transition metals [11]; thus, aggregation of the metal into nanoparticles is expected to suppress the effects of substrate polarization on catalytic activity. In this work, we attempt to mitigate these challenges by considering the use of a ferroelectric substrate to tune the surface properties of thin films of an insulating catalytic oxide. In particular, we use DFT to investigate the surface chemistry of thin $\text{ZnO}(11\bar{2}0)$ films supported on ferroelectric PbTiO_3 .

Zinc oxide is commonly used as a catalyst for the industrially and environmentally important CO and CO_2 conversion reactions, frequently in conjunction with a copper co-catalyst [12–15]. Therefore the properties of the various ZnO surface terminations have been extensively studied [16–19]. We choose to study the epitaxial interface of non-polar $\text{ZnO}(11\bar{2}0)$ films with PbTiO_3 (PTO), as similar systems have previously been grown. Wei *et. al.* [20] reported heteroepitaxial growth of $\text{ZnO}(11\bar{2}0)$ on $\text{SrTiO}_3(001)$ and $\text{BaTiO}_3(001)/\text{SrTiO}_3(001)$ surfaces, suggesting that $\text{PbTiO}_3(001)$, which has the same crystal structure and very similar in-plane lattice constant, will also provide an experimentally feasible substrate for $\text{ZnO}(11\bar{2}0)$ films.

To investigate the $\text{ZnO}(11\bar{2}0)/\text{PbTiO}_3(001)$ heterostructure, we perform DFT computations using the plane-wave pseudopotential code Quantum Espresso [21] with ultrasoft pseudopotentials [22] and a 35Ry energy cutoff. The Wu-Cohen GGA functional [23] is used to de-

scribe exchange correlation; this functional has been shown to have equivalent or better performance to the ubiquitous PBE GGA functional for the prediction of structural and energetic properties of ferroelectric perovskite oxides, as well as a range of other solids, surfaces, and molecules [24].

To model the heterostructure, we use the experimentally reported $\text{ZnO}(11\bar{2}0)/\text{SrTiO}_3(001)$ epitaxial relationship [20]. The PbO-termination of the $\text{PbTiO}_3(001)$ slabs is selected, as this has been demonstrated to be the thermodynamically favored slab termination under relevant conditions [25]. Below, we use the notation $(\text{ZnO})_n/\text{PbTiO}_3\uparrow$ and $(\text{ZnO})_n/\text{PbTiO}_3\downarrow$ for $\text{ZnO}(11\bar{2}0)$ grown on positively polarized (“up”) and negatively polarized (“down”) $\text{PbTiO}_3(001)$ slabs, respectively, where n is the number of $\text{ZnO}(11\bar{2}0)$ atomic layers. The supercell geometry is illustrated in Fig. 1. A PbO-terminated cell with nine alternating PbO and TiO_2 atomic layers stacked in the (001) direction is used to represent the ferroelectric PbTiO_3 substrate. For calculations without CO_2 adsorption or dissociation, we use a $c(2\times 2)$ PTO cell for which a $4\times 4\times 1$ k -point mesh is sufficient. For other calculations, we use a (2×2) PTO cell. A 20Å vacuum was added between periodic images in the z -direction and a dipole correction [26] is applied in the center of the vacuum region to remove artificial fields between periodic images in all calculations.

We first investigate possible thermodynamic ground states of the heterostructure under excess oxygen as would be expected during growth and device operation. Figure 2 is a plot of the free energy of formation for inserting an oxygen into the space created at the interface by the unmatched stacking of atomic layers. Our results show that under growth regular conditions ($T=400\text{--}700^\circ\text{C}$ and $P=10^{-5}\text{Pa}$ [20] at which $\mu_{\text{O}} \approx -1.1 - 1.5\text{eV}$) an extra oxygen will remain at the interface when the substrate is positively polarized. On the negatively polarized structure, this non-stoichiometric structure

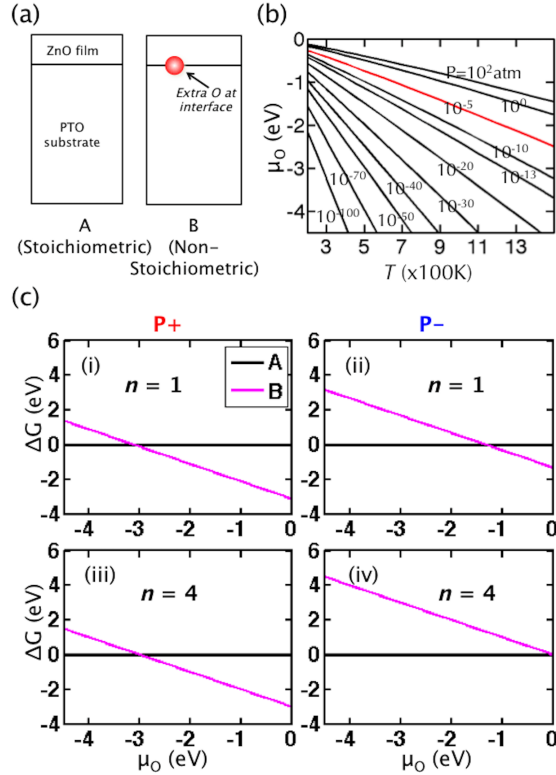


FIG. 2. (a) Possible configurations in an oxygen-rich environment. (b) Oxygen chemical potential as a function of temperature and pressure. (c) Free energy versus oxygen chemical potential for $n = 1$ and $n = 4$. shaded regions represent the range of μ_O under the growth conditions reported in Ref. [20] is 10^{-5} Pa (highlighted line) and $400^\circ\text{C} < T < 700^\circ$. μ_O can be decreased by reducing pressure and increasing temperature.

is only stable at lower temperatures.

In order to decide whether or not the structure with an extra oxygen is relevant for our CO_2 dissociation calculations, we perform calculations for the energy required to have an oxygen vacancy in each ZnO layer in the 4-layer-thick supported-ZnO case. Figure 3(a), which shows the O vacancy formation energy in each layer for this film, suggests that after a number of layers have been grown, the configuration at the interface will be maintained irrespective of

the thermodynamic stability of the structure. If an oxygen is already trapped at the interface (for example, if the film is grown over a positively polarized substrate and the polarization was later switched), its removal will involve a series of steps that include the removal of one of the topmost oxygen atoms. Given the high vacancy formation energies of $\sim 3.5\text{eV}$, this process will be kinetically limited. Conversely, if there is no oxygen at the interface (for example, growing the under a negatively polarized substrate and the polarization was later switched), oxygen insertion will involve one of the oxygen atoms in the lowest ZnO layer moving to the interfacial O location and leaving behind a vacancy. In our calculations, we do not observe a stable system with this configuration.

However, the above considerations do not take into account the effect of other gas phase molecules in the environment. For CO_2 dissociation, for example, CO adsorption also occurs. Our calculations show that if an oxygen atom exists at the interface, it can be easily removed by adsorption of a CO molecule, as illustrated in figure 3(b) for $n = 1$ and 2. This suggests an interesting application of non-stoichiometric $(\text{ZnO})_n/\text{PbTiO}_3$ for small n : catalytic oxidation of CO to CO_2 , since interface stability dictates that the non-stoichiometric interface will exist as long as there is O_2 gas in the atmosphere at most conditions encountered in practice, and this structure easily oxidizes CO.

The foregoing also suggests that it is possible to obtain a stoichiometric interface if the ZnO thin film is grown at the negatively-polarized structure under conditions of lower oxygen partial pressure and/or higher temperature (i.e., lower oxygen chemical potential, μ_O). This configuration will be trapped when the polarization of the substrate is switched with an electric field. In the following, we perform calculations to explore CO_2 dissociation on the surfaces of this structure as a function of polarization direction and ZnO film thickness. We then show that a dynamically tunable scheme using this heterostructure can enable a much lower over-

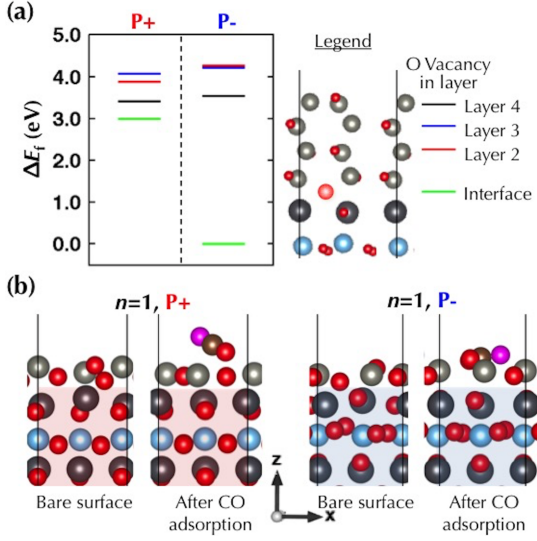


FIG. 3. (a) Oxygen vacancy formation energy, ΔE_f , as a function of distance from the interface. The presence of an extra O at the interface is predicted to be determined by the initial growth configuration. (b) Atomic structure of CO on the non-stoichiometric $(\text{ZnO})_1/\text{PbTiO}_3\uparrow$ and $(\text{ZnO})_1/\text{PbTiO}_3\downarrow$, demonstrating the selective removal of interfacial O by the adsorbing CO. Atom colors are the same as in Fig. 1, with adsorbate O atoms shown in magenta for clarity.

all activation energy for the CO_2 dissociation process.

We perform calculation of the adsorption energies of CO_2 and $\text{CO} + \frac{1}{2}\text{CO}_2$ on the surfaces using a coverage of one molecular adsorbate per 2×2 PbTiO_3 surface cell, starting from a range of initial adsorbate positions and geometries. The reported adsorption energies in Fig. 4(a) are for the minimum energy adsorption geometry on the indicated surface. As the figure demonstrates, changing the polarization direction of the substrate leads to a difference of $\sim 0.6\text{eV}$ in the CO_2 adsorption energy for the thinnest ZnO film. The results demonstrate the changing surface chemistry as a function of substrate polarization and film thickness. The difference tapes off, with the heterostructure behaving very similarly to the unsupported ZnO

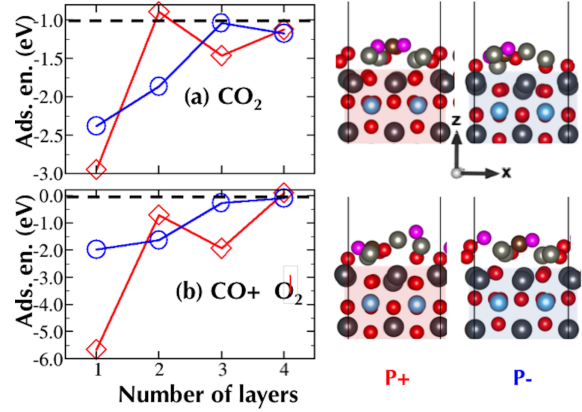


FIG. 4. Adsorption energies of (a) CO_2 , and (b) $\text{CO} + \frac{1}{2}\text{O}_2$, on $(\text{ZnO}(11\bar{2}0))_n/[2 \times 2]\text{PbTiO}_3$ as a function of n . Diamonds and circles represent adsorption on the positively and negatively polarized structures, respectively. Horizontal dashed lines represent the adsorption energy of the molecules on an unsupported ZnO slab. Structures on the right show the adsorption configurations for the corresponding molecule on stoichiometric structures with $n=1$. Oxygen atoms in the adsorbates are colored magenta for clarity.

slab for $n \geq 4$ ZnO layers. Similar behavior is seen for $\text{CO} + \frac{1}{2}\text{CO}_2$, as shown in Fig. 4(b).

The flip-flop pattern in the adsorption energies in the plots in Fig. 4 can be directly correlated to the cation displacements at the slab surface, which has the same form with respect to number of ZnO layers and substrate polarization (see the supplemental material [27]). We find that the magnitude of the displacement in each ZnO layer depends on the distance from the PbTiO_3 surface and its polarization, becoming approximately the same as that in surface of the unsupported thick ZnO after the third layer for both substrate polarization directions. In other words, the magnitude and degree of decay of the surface zinc-oxygen displacements away from the substrate are directly related to the dipole at the interface. Therefore, by changing the magnitude of the displacement at the interface, it may be possible to modify the displacement at the ZnO surface and thus the sensitiv-

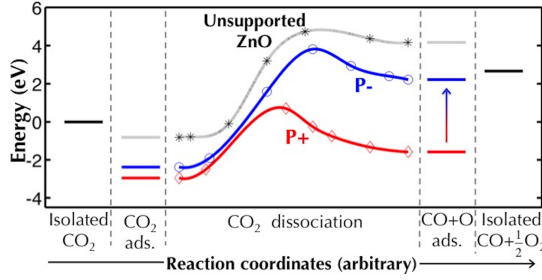


FIG. 5. Reaction pathway for CO_2 dissociation over unsupported ZnO (gray stars) and ZnO supported on positively and negatively poled PbTiO_3 (red diamonds and blue circles, respectively). The vertical axis is energy with respect to an isolated CO_2 molecule. The vertical arrow indicates switching of the substrate polarization from P+ to P-.

ity of the tunable catalyst. To confirm this hypothesis, we perform calculations using the less stable [28] TiO_2 -terminated surface, which exhibits smaller displacements than the PbO termination. We find that CO_2 adsorption on one-layer of ZnO supported on the TiO_2 -terminated substrate is $\sim 10\%$ ($\sim 54\%$) as strong as that on the positively (negatively) polarized PbO -terminated substrate, suggesting that an important design principle for a tunable catalyst with ZnO is to find substrates with reversible polarizations and large surface displacements. We predict, for example, that the ferroelectricity-induced ZnO surface chemistry changes will be greater for BiMO_3 than BaTiO_3 or PbTiO_3 substrates.

As adsorption energy [29, 30], adsorption geometry [31], and surface charges (dipoles) [32] all affect reaction pathways and energetics, our results strongly suggest that the polarization-induced changes in these properties will affect CO_2 conversion processes. We investigate this idea further by determining the reaction pathway and energy barrier for a simple conversion process: thermally-activated dissociation of $\text{CO}_2(\text{g})$ into $\text{CO}(\text{g})$ and $\text{O}_2(\text{g})$ over a reversibly tunable surfaces of $(\text{ZnO})_n/\text{PbTiO}_3$. To compute the energy along the reaction path-

way for each system, we use nudged elastic band calculations [33, 34] to determine the reaction pathways. Figure 5 shows the computed reaction pathways for $\text{CO}_2(\text{g})$ adsorption and conversion to $\text{CO}(\text{g})$ and $\text{O}_2(\text{g})$ over the ferroelectric-supported ZnO films with $n = 1$ and on the unsupported ZnO(11 $\bar{2}$ 0) slab. The first step of the reaction, CO_2 adsorption, is a spontaneous process on all three surfaces. The dissociation of adsorbed CO_2 into adsorbed CO and adsorbed O is endothermic for all three surfaces, but is significantly more favorable on the positively polarized structure (red line), with an activation energy barrier less than half that of the reference unsupported ZnO slab (dashed line). The last step, desorption of $\text{CO} + \frac{1}{2}\text{O}_2$, however requires a large energy input for the positively polarized structure, but occurs spontaneously for the reference surface and requires only minimal energy for the negatively polarized structure.

Our results suggest a possible approach for increasing the rate of CO_2 dissociation on ZnO surfaces: grow a ZnO thin film on a positively polarized substrate, on which the first few steps of the reaction take place, switch the polarization (depicted by the arrow in the figure) to induce the desorption of the products, then switch back and repeat. Using a quasi-equilibrium approximation (see supplemental material [27]), our calculations show that the dynamic switching scheme will result in 10-20 orders of magnitude increase in reaction rates compared to the dissociation on the unsupported slab. Also, at a given rate, the reaction on the tunable catalyst proceeds at less than half of the temperature required for the process on the unsupported slab. These results clearly demonstrate the potential advantages of dynamically switching the surface properties of a catalyst to enhance the turnover of a product.

In conclusion, we have shown that the configuration at the interface is dependent on the growth conditions and polarization of the substrate. We also show that the surface chemistry of stoichiometric $(\text{ZnO}(11\bar{2}0))_n/\text{PbTiO}_3$

is dependent on both the polarization direction of the PbTiO_3 substrate and the number of $\text{ZnO}(11\bar{2}0)$ layers n , with the effect of the substrate polarization becoming negligible for $n \geq 4$. The large changes in CO_2 adsorption energy with polarization switching reported in this work suggest the possibility of controlling reaction energetics and pathways of CO_2 reactions, as indicated by the proposed dynamic polarization-switching scheme for a CO_2 dissociation reaction on $\text{ZnO}(11\bar{2}0)/\text{PbTiO}_3$. Finally, we note that this approach can be applied to many other reactions in heterogeneous catalysis, potentially opening new avenues for controlling reaction energetics.

This work was supported by an MIT Energy Initiative seed grant. We gratefully acknowledge the use of computing resources from NERSC and TACC. We appreciate stimulating discussions with Dr. Brian Kolb about this work.

* Corresponding author.

kolpak@mit.edu

Present address: 77 Massachusetts Avenue, rm 3-156, Cambridge, MA 02139, USA.

- [1] R. S. Haszeldine, *Science* **325**, 1647 (2009), <http://www.sciencemag.org/content/325/5948/1647.full.pdf>.
- [2] M. Peters, B. Khlér, W. Kuckshinrichs, W. Leitner, P. Markewitz, and T. E. Müller, *ChemSusChem* **4**, 1216 (2011).
- [3] H. L. Stadler, *Physical Review Letters* **14**, 979–981 (1965).
- [4] G. Parravano, *The Journal of Chemical Physics* **20**, 342–342 (1952).
- [5] K. Garrity, A. M. Kolpak, S. Ismail-Beigi, and E. I. Altman, *Advanced Materials* **22**, 2969 (2010).
- [6] A. Kakekhani and S. Ismail-Beigi, *ACS Catalysis* **0**, 4537 (0), <http://dx.doi.org/10.1021/acscatal.5b00507>.
- [7] A. Riefer, S. Sanna, and W. G. Schmidt, *Phys. Rev. B* **86**, 125410 (2012).
- [8] D. Li, M. H. Zhao, J. Garra, A. M. Kolpak, A. M. Rappe, D. A. Bonnell, and J. M. Vohs, *Nat Mater* **7**, 473 (2008).
- [9] C. Baeumer, D. Saldana-Greco, J. M. P. Martinez, A. M. Rappe, M. Shim, and L. W. Martin, *Nat Commun* **6** (2015), 10.1038/ncomms7136.
- [10] A. M. Kolpak, I. Grinberg, and A. M. Rappe, *Physical Review Letters* **98**, 166101 (2007).
- [11] C. T. Campbell, *Surface Science Reports* **27**, 1 (1997).
- [12] M. Behrens, F. Studt, I. Kasatkin, S. Kuhl, M. Havecker, F. Abild-Pedersen, S. Zander, F. Girgsdies, P. Kurr, B.-L. Kniep, M. Tovar, R. W. Fischer, J. K. Nørskov, and R. Schlögl, *Science* **336**, 893 (2012).
- [13] J.-D. Grunwaldt, A. Molenbroek, N.-Y. Topse, H. Topse, and B. Clausen, *Journal of Catalysis* **194**, 452 (2000).
- [14] I. Kasatkin, P. Kurr, B. Kniep, A. Trunschke, and R. Schlögl, *Angewandte Chemie* **119**, 7465 (2007).
- [15] K. Ernst, A. Ludviksson, R. Zhang, J. Yoshihara, and C. Campbell, *Phys. Rev. B* **47**, 13782 (1993).
- [16] M. Kurtz, J. Strunk, O. Hinrichsen, M. Muhler, K. Fink, B. Meyer, and C. Woll, *Angewandte Chemie International Edition* **44**, 2790 (2005).
- [17] Y. R. Wang and C. B. Duke, *Surface science* **192**, 309–322 (1987).
- [18] B. Meyer and D. Marx, *Physical Review B* **67** (2003).
- [19] J. Kößmann, G. Roßmüller, and C. Hattig, *The Journal of Chemical Physics* **136**, 034706 (2012).
- [20] X. H. Wei, Y. R. Li, W. J. Jie, J. L. Tang, H. Z. Zeng, W. Huang, Y. Zhang, and J. Zhu, *Journal of Physics D: Applied Physics* **40**, 7502 (2007).
- [21] Paolo Giannozzi, Stefano Baroni, Nicola Bonini, Matteo Calandra, Roberto Car, Carlo Cavazzoni, Davide Ceresoli, Guido L Chiarotti, and Matteo Cococcioni, *Journal of Physics: Condensed Matter* **21**, 19 (2009).
- [22] D. Vanderbilt, *Physical Review B* **41**, 7892 (1990).
- [23] Z. Wu and R. E. Cohen, *Physical Review B* **73**, 235116 (2006).
- [24] F. Tran, R. Laskowski, P. Blaha, and K. Schwarz, *Physical Review B* **75** (2007).
- [25] K. Garrity, A. Kakekhani, A. Kolpak, and S. Ismail-Beigi, *Physical Review B* **88**, 045401 (2013).
- [26] L. Bengtsson, *Physical Review B* **59**, 12301 (1999).

- [27] See the Supplemental Material for an investigation of the need for a bottom electrode in describing the surface properties of the systems of interest, details of the mechanism of interface-mediated surface chemistry and the derivation of the formulae for the rate of CO₂ dissociation.
- [28] K. Garrity, A. Kakekhani, A. Kolpak, and S. Ismail-Beigi, *Phys. Rev. B* **88**, 045401 (2013).
- [29] A. Michaelides, Z.-P. Liu, C. J. Zhang, A. Alavi, D. A. King, and P. Hu, *Journal of the American Chemical Society* **125**, 3704 (2003), <http://dx.doi.org/10.1021/ja027366r>.
- [30] T. Bligaard, J. Norskov, S. Dahl, J. Matthiesen, C. Christensen, and J. Sehested, *Journal of Catalysis* **224**, 206 (2004).
- [31] N. A. Ramsahye, G. Maurin, S. Bourrelly, P. L. Llewellyn, C. Serre, T. Loiseau, T. Devic, and G. Férey, *The Journal of Physical Chemistry C* **112**, 514 (2008).
- [32] J. H. Lee and A. Selloni, *Phys. Rev. Lett.* **112**, 196102 (2014).
- [33] G. Henkelman, B. P. Uberuaga, and H. Jónsson, *The Journal of Chemical Physics* **113**, 9901–9904 (2000).
- [34] D. Sheppard, R. Terrell, and G. Henkelman, *The Journal of Chemical Physics* **128**, 134106 (2008).

Supplemental Material for PbTiO₃(001) Capped with ZnO(11 $\bar{2}$ 0): An Ab-Initio Study of Effect of Substrate Polarization on Interface Composition and CO₂ Dissociation

Babatunde Alawode and Alexie Kolpak*
Massachusetts Institute of Technology, Cambridge, MA 02139

EFFECT OF ADDING AN ELECTRODE

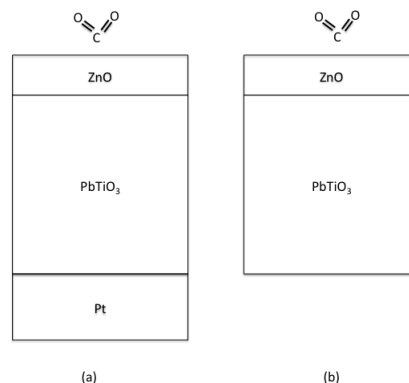
An electrode or some kind of support is necessary for most applications involving perovskites. Electrodes have been demonstrated to have significant effects on the perovskite properties. For example, Sai *et al* [S1] reported that the Pt electrodes cancel 97% of the depolarizing field in thin PbTiO₃ thin films and thus help to maintain some polarization even in films one lattice unit thick. The grounded electrodes provides metallic screening that compensates the polarization charge. Arras *et al.* [S2] carried out an interesting study on the effects of metal electrodes on the LaAlO₃/SrTiO₃ interface. They showed that changing the type of metal greatly affects the Schottky barrier, carrier concentration and lattice polarization at the interface.

In the light of these, it is imperative to understand how adding a metal electrode in our model of the ZnO/PbTiO₃ affects the ZnO surface (hence catalytic) properties. If the electrode has an effect, we will have a better understanding of phenomena at the surfaces. If it does not, then we can get away with modeling a ZnO/PbTiO₃ system with fewer atoms hence less computational costs.

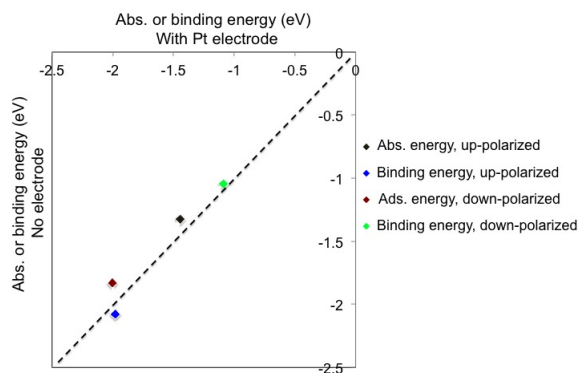
We use two ZnO layers, four lattice parameter thick PbO-terminated PbTiO₃ slab (bottom three fixed) and four layers of Pt at the bottom. We calculate the ZnO binding energy PbTiO₃/Pt and PbTiO₃, density of states of ZnO/PbTiO₃/Pt and ZnO/PbTiO₃, and CO₂ adsorption energy on ZnO/PbTiO₃/Pt and ZnO/PbTiO₃. With the Pt and ZnO layers and the top-most PbTiO₃ layer relaxed, we calculate the binding energy of ZnO to PbTiO₃ in the presence and absence of the electrode. We find that the electrode has no effect of the ZnO binding or CO₂ adsorption. The results are presented in Fig. S1.

Finally, we examine whether an electrode affects the electronic structure of the surface. As seen in Fig. S2, there is no significant change in the electronic structure of the layer both for the up- and down- polarized catalyst when the platinum electrode is removed.

From the foregoing, it is evident the electrode is not important to consider. Therefore, in this work, we model ZnO/PbTiO₃/Pt as ZnO/PbTiO₃.



(a) Schematic



(b) Results

FIG. S1: (a) Determining the effects of platinum electrodes on surface properties. Calculations were carried out with an electrode support and without an electrode support. (b) Comparing the ZnO binding energy on PbTiO₃ and CO₂ adsorption energy on ZnO/PbTiO₃ with and without a Pt electrode.

MECHANISM FOR INTERFACE-MEDIATED SURFACE CHEMISTRY

An inspection of the relaxed configuration of the heterostructures show changes in the surface Zn-O displacements with respect to the unsupported slab. The mechanism for this is shown illustrated in Fig. S3(a) and (b). The attraction of the Pb atoms on the substrate side at

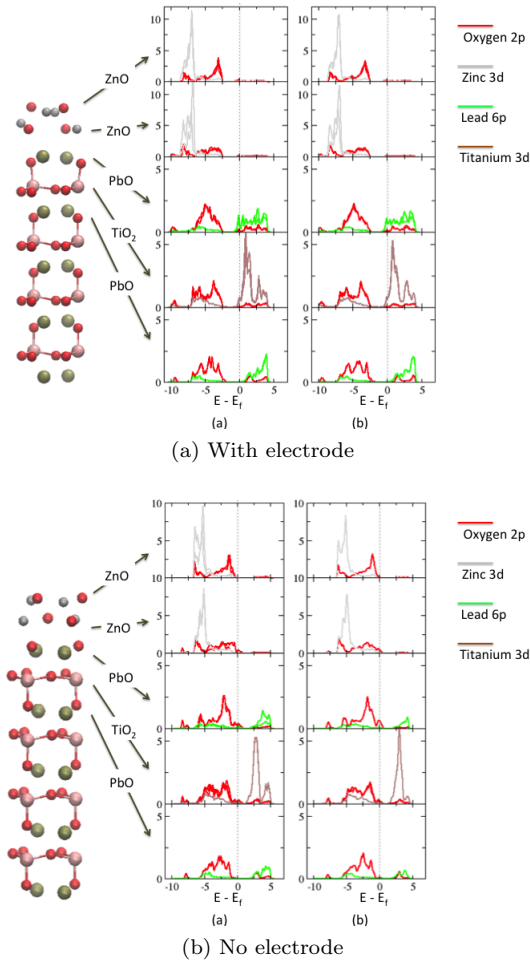


FIG. S2: Projected densities of states for the topmost five layers of a) (ZnO)₂/PbTiO₃/Pt and b) (ZnO)₂/PbTiO₃.

the interface of the positively-polarized structure to the O atoms in the ZnO film causes an increase in the Zn-O displacement in that layer. The next layer however experiences a decrease in its Zn-O displacement, and so on. The opposite effect explains the trend for the negatively polarized structure. The effect of the interface mediation gets weaker as the surface layers gets farther from the surface. The data plotted Fig. S3(c) suggests that the interface mediated mechanism is correct.

RATE EQUATION FOR CO₂ DISSOCIATION ON ZNO AND ZNO/PBTIO₃

Step 1 (CO₂ adsorption): CO₂ + 3 * → CO₂ ***

Step 2 (CO₂ dissociation): CO₂ *** → CO ** + O* .

This is the rate limiting step

Step 3 (CO desorption): CO ** + O* → CO + 2 * + O*

Step 4 (Oxygen desorption): O* → 1/2 O₂ + *

We apply quasi-static approximation (all steps except

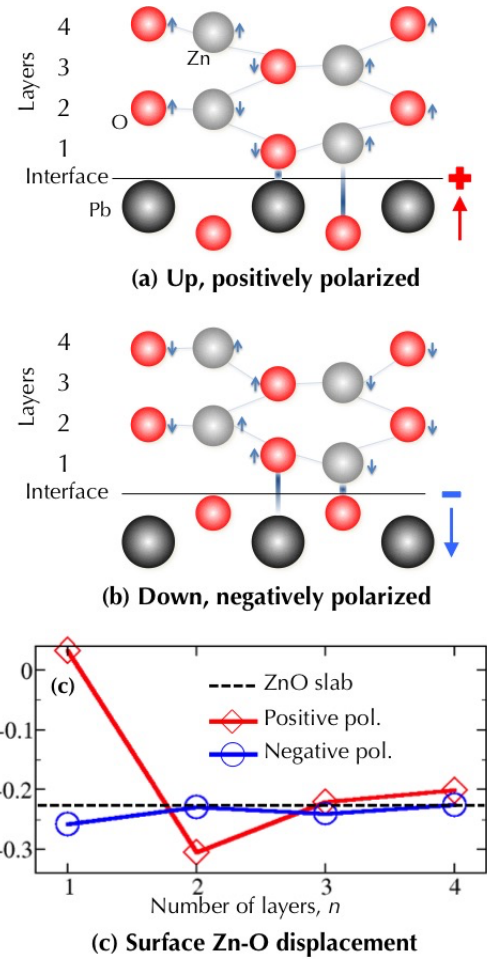


FIG. S3: Mediation of the interface chemistry by the (a) positively polarized (b) negatively polarized substrates. (c) is a plot of the surface displacements.

the rate limiting step are in equilibrium). We define the rate constants for each step.

$$K_1 = \frac{\theta_{\text{CO}_2}}{\frac{P_{\text{CO}_2}}{P_{\text{ref}}} \theta_*^3} \quad (\text{S1})$$

$$K_2 = \frac{\theta_{\text{CO}} \theta_{\text{O}}}{\theta_{\text{CO}_2}} \quad (\text{S2})$$

$$K_3 = \frac{\theta_*^2 \frac{P_{\text{CO}}}{P_{\text{ref}}}}{\theta_{\text{CO}}} \quad (\text{S3})$$

$$K_4 = \frac{\theta_* \left(\frac{P_{\text{O}_2}}{P_{\text{ref}}} \right)^{1/2}}{\theta_{\text{O}}} \quad (\text{S4})$$

The coverages θ are related by:

$$\theta_{\text{CO}_2} + \theta_{\text{CO}} + \theta_{\text{O}} + \theta_* = 1$$

which gives

$$K_4 = e^{-\Delta G_4/kT}$$

$$K_1 \left(\frac{P_{O_2}}{P_{ref}} \right) \theta_*^3 + \frac{1}{K_3} \left(\frac{P_{CO}}{P_{ref}} \right) \theta_*^2 + \frac{1}{K_4} \left(\frac{P_{CO}}{P_{ref}} \right)^{1/2} \theta_* + \theta_* = 1 \quad (S5)$$

We can find the coverages by solving this equation.

The overall rate of reaction, in number of CO₂ converted per second, is given by the rate of the limiting step

$$\begin{aligned} R_{overall} = R_2 &= k_2 \theta_{CO_2} - k_{-2} \theta_O \theta_{CO} \\ &= k_2 \theta_{CO_2} - \frac{k_{-2}}{K_2} \theta_O \theta_{CO} \\ &= k_2 \theta_{CO_2} - k_2 \theta_{CO_2} \frac{\theta_O \theta_{CO}}{K_2 \theta_{CO_2}} \\ &= k_2 \theta_{CO_2} (1 - \beta) \\ &= k_2 K_1 \left(\frac{P_{CO_2}}{P_{ref}} \right) \theta_*^3 (1 - \beta) \end{aligned}$$

where β is the approach to equilibrium for the rate limiting step.

In the final expression, we note that:

$$\beta = \frac{\theta_O \theta_{CO}}{K_2 \theta_{CO_2}}$$

$$k_2 = v_2 e^{-E_a/kT}$$

$$K_1 = e^{-\Delta G_1/kT}$$

$$K_3 = e^{-\Delta G_3/kT}$$

where v_2 is the attempt frequency, k_2 and E_a are the rate constant and activation energy of the forward reaction for the RLS respectively, and K_1 , K_3 and K_4 are the equilibrium constants of the corresponding steps.

The rate of reaction, in g/s is then given by:

$$R_{mass} = M_{CO_2} * R_{overall} * A_s * N_s / N_A$$

where R_{mass} , M_{CO_2} , A_s , N_s and N_A are the mass flow rate in g/s, molar mass of CO₂, number of sites available per area and the Avogadro number respectively. Solving these equations at fixed values of effective surface area $A_s = 2 \times 10^7 \text{m}^2$, CO₂ partial pressure of 2atm, a frequency factor of 5×10^{13} and $\beta = 0.5$ yields the results reported in the paper. Varying these values over a wide range do not significantly affect the results since we are concerned with the ratio of the rates.

* Corresponding author.

kolpak@mit.edu

Present address: 77 Massachusetts Avenue, rm 3-156, Cambridge, MA 02139, USA.

[S1] N. Sai, A. M. Kolpak, and A. M. Rappe, Physical Review B **72**, 020101 (2005), URL <http://link.aps.org/doi/10.1103/PhysRevB.72.020101>.

[S2] R. Arras, V. G. Ruiz, W. E. Pickett, and R. Pentcheva, Physical Review B **85**, 125404 (2012), URL <http://link.aps.org/doi/10.1103/PhysRevB.85.125404>.